

Microfluidic assay of the deformability of primitive erythroblasts

Sitong Zhou, Yu-Shan Huang, Paul D. Kingsley, Kathryn H. Cyr, James Palis, and Jiandi Wan

Citation: *Biomicrofluidics* **11**, 054112 (2017); doi: 10.1063/1.4999949

View online: <https://doi.org/10.1063/1.4999949>

View Table of Contents: <http://aip.scitation.org/toc/bmf/11/5>

Published by the [American Institute of Physics](#)

Articles you may be interested in

[Particle separation by phase modulated surface acoustic waves](#)

Biomicrofluidics **11**, 054115 (2017); 10.1063/1.5001998

[A compact microfluidic chip with integrated impedance biosensor for protein preconcentration and detection](#)

Biomicrofluidics **11**, 054113 (2017); 10.1063/1.4996118

[Advances in microfluidic devices made from thermoplastics used in cell biology and analyses](#)

Biomicrofluidics **11**, 051502 (2017); 10.1063/1.4998604

[Localization of low-abundant cancer cells in a sharply expanded microfluidic step-channel using dielectrophoresis](#)

Biomicrofluidics **11**, 054114 (2017); 10.1063/1.4998756

[Design considerations for open-well microfluidic platforms for hypoxic cell studies](#)

Biomicrofluidics **11**, 054116 (2017); 10.1063/1.4998579

[A fast and efficient size separation method for haploid embryonic stem cells](#)

Biomicrofluidics **11**, 054117 (2017); 10.1063/1.5006326

Looking for a specific
instrument?



Easy access to the latest equipment.
Shop the *Physics Today* Buyer's Guide.

PHYSICS
TODAY

lasers imaging
VACUUM EQUIPMENT
instrumentation
software MATERIALS
cryogenics
+ MORE...

Microfluidic assay of the deformability of primitive erythroblasts

Sitong Zhou,¹ Yu-Shan Huang,² Paul D. Kingsley,³ Kathryn H. Cyr,⁴
 James Palis,^{2,3} and Jiandi Wan^{1,5,6,a)}

¹*Microsystems Engineering, Rochester Institute of Technology, Rochester, New York 14623, USA*

²*Department of Biomedical Genetics, University of Rochester, Rochester, New York 14642, USA*

³*Department of Pediatric and Center for Pediatric Biomedical Research, University of Rochester, Rochester, New York 14642, USA*

⁴*Department of Biomedical Engineering, Rochester Institute of Technology, Rochester, New York 14623, USA*

⁵*Center for Translational Neuromedicine, University of Rochester Medical Center, Rochester, New York 14642, USA*

⁶*Department of Biomedical Engineering, University of Rochester, Rochester, New York 14627, USA*

(Received 11 August 2017; accepted 4 October 2017; published online 23 October 2017)

Primitive erythroblasts (precursors of red blood cells) enter vascular circulation during the embryonic period and mature while circulating. As a result, primitive erythroblasts constantly experience significant hemodynamic shear stress. Shear-induced deformation of primitive erythroblasts however, is poorly studied. In this work, we examined the deformability of primitive erythroblasts at physiologically relevant flow conditions in microfluidic channels and identified the regulatory roles of the maturation stage of primitive erythroblasts and cytoskeletal protein 4.1 R in shear-induced cell deformation. The results showed that the maturation stage affected the deformability of primitive erythroblasts significantly and that primitive erythroblasts at later maturational stages exhibited a better deformability due to a matured cytoskeletal structure in the cell membrane. *Published by AIP Publishing.*
<https://doi.org/10.1063/1.4999949>

I. INTRODUCTION

Primitive erythroblasts are precursors of erythrocytes (otherwise known as red blood cells) and essential to the regeneration of erythrocytes and fetal development. Unlike the definitive erythropoiesis, which is observed in the fetal liver and the postnatal bone marrow, primitive erythroblasts are only found in the embryo.^{1–3} Primitive erythroblasts carry both embryonic and adult hemoglobin while “definitive” cells only accumulate adult hemoglobin.^{2,3,7,8} The primitive erythroid lineage arises in the yolk sac, as pools of immature erythroblasts in “blood islands” are first apparent in the murine embryo at the embryonic day of 7.25–7.5 (E7.0–7.5).¹ The number of primitive erythroid cells increases significantly within a vascular plexus at E8.0.^{1,4} Different from definitive cells that enter the circulation after maturation, these large, immature, nucleated primitive cells move into the distal region of yolk sac and enter circulation beginning at E8.25, with the onset of cardiac contractions.^{1–8} Similar to the process in mouse, nucleated primitive erythroblasts join the yolk-sac circulation from the fourth to fifth week of gestation in humans. Primitive erythroblasts can be further identified in the embryo after 6 weeks.⁸ Starting from the eighth week, definitive cells from the liver are observed while primitive erythroblasts are still the majority.⁸ Due to the similar maturation

^{a)} Author to whom correspondence should be addressed: jdween@rit.edu

process of primitive erythroblasts in humans and mouse, many studies of primitive erythroblasts are conducted in mouse embryos.

In mouse embryo, primitive erythroblasts mature as a semi-synchronous cohort over the next several days as they circulate in the bloodstream. Primitive erythroblasts transit from proerythroblasts at E9.5 to orthochromatic erythroblasts at E12.5 and then enucleate over the subsequent 4 days of gestation^{2,4} to produce mature erythrocytes. The circulation of primitive erythroblasts also contributes to the formation and remodeling of blood vessels in the yolk sac. Without the presence of such circulation, for example, regular development of the embryo such as vessel remodeling and maturation is impaired.^{9–11} Primitive erythroblasts experience shear stresses in the fetal bloodstream and have to move throughout the embryonic microvasculature that has a diameter from 4 to 60 μm .¹² Because the size of primitive erythroblasts with maturation stages from E8.5 to E12.5 varies from 17 μm to 13 μm ,¹³ flexibility and elasticity that allow the primitive erythroid cells to move through the embryonic microvasculature are crucially important. Although the structure and composition of the cytoskeletal network in adult erythrocytes, as well as their deformability, are well established, the deformability of maturing erythroblast precursors is less understood. One of the possible reasons is that protein composition in the cytoskeleton of primitive erythroblasts changes with the maturation stage. Decreases in surface area (about a 35% loss), volume (50% loss), and sphericity (6% loss) along maturation have been observed and can be attributed to the membrane and cytoskeleton protein remodeling.¹⁴ Remodeling also leads to a reduced stiffness of the cell membrane.¹⁴ In addition, as primitive erythroblasts mature, shear stress activates intracellular kinases to remodel the membrane and cytoskeletal compositions.¹⁰ Without the correct protein components that make up the cytoskeleton network such as actin, spectrin, and protein 4.1R,¹⁵ erythroid cells will have a less deformable cytoskeleton network that could potentially lead to hemolytic anemia.¹⁶

While the structural remodeling of the membrane and cytoskeleton of primitive erythroblasts has been investigated, flow-induced deformation of primitive erythroblasts at different maturation stages is less studied. In addition, although defects of protein 4.1 R are tightly linked to hereditary elliptocytosis,¹⁷ characterized by morphologically abnormal and mechanically unstable erythrocytes,^{18–24} the regulatory role of protein 4.1 R in erythroblast deformation remains unknown.

Although studies of deformability-induced red cell migration have been conducted in small capillaries under a bulk suspension,^{25,26} we here developed microfluidic approaches to study the deformability of single primitive erythroblasts under physiologically relevant flow conditions. We determined the effect of maturation stage on the deformability of primitive erythroblasts and unveiled the regulatory roles of protein 4.1 R in cell deformation. Last, we investigated the deformability of primitive erythroblasts when squeezing through a narrow constriction channel mimicking the size of the capillary.

II. EXPERIMENTAL METHODS

A. Mice and collection of embryonic peripheral blood

All animal experiments were approved by the University of Rochester Committee on Animal Resources (UCAR). *Epb4.1*^{+/+} and *Epb4.1*^{-/-} mice¹⁷ were provided by Dr. John Conboy (Life Sciences Division, Lawrence Berkeley National Laboratory, Berkeley, CA).

Outbred ICR (Taconic Biosciences, Germantown, NY) and *Epb4.1*^{+/-} mice were mated overnight, and vaginal plugs were checked the following morning (embryonic day 0.3; E0.3). At defined gestational ages, mice were sacrificed by CO₂ narcosis and the embryos were dissected in PB2^{27,28} containing 12.5 $\mu\text{g}/\text{ml}$ of heparin. E10.5 and E12.5 embryos were bled in PB2 and the embryonic peripheral blood was collected from the bottom of the dishes. Total cell numbers and viability were determined by trypan blue staining (Sigma-Aldrich). Embryos from *Epb4.1*^{+/-} mouse mating were genotyped using the AccuStartTM II Mouse Genotyping Kit (Quanta Biosciences) with primer pairs as follows: neo (neo-f, 5'-GATGGATTGCACGCAGGT-3'; neo-r, 5'-GGCAGGAGCAAGGTGAGA-3'; 318 bp);²⁹ *Epb 4.1* exon 4 (Epb4.1E4-f,

5'-GCTCAGGAAGAACACAGAGAGG-3'; Epb4.1E4-r, 5'-CATTCGTAGACCGTGTCCATCC-3'; 197 bp).²⁹

B. Microfluidic fabrication and experimental setup

Polydimethylsiloxane (PDMS) chips were fabricated using standard soft photolithography techniques. The channel inside of the PDMS chip has a uniform length of $100\ \mu\text{m}$ ($l_c = 100\ \mu\text{m}$) and a width of $20\ \mu\text{m}$ ($w_c = 20\ \mu\text{m}$) at a constriction section, and a width of $100\ \mu\text{m}$ for the rest of the channel. The height of the channel is $30\ \mu\text{m}$ ($h = 30\ \mu\text{m}$) everywhere. To test the deformability in a narrow microfluidic channel, we fabricated a microfluidic channel with $l_c = 170\ \mu\text{m}$, $w_c = 5\ \mu\text{m}$, and $h = 7\ \mu\text{m}$, which mimics the size of capillaries.¹² Using a 1 mL syringe and needle (Med Lab Supply), the suspension of primitive erythroblasts collected from mouse embryos (2 v/v % in PBS) was transferred to polyethylene tubing [Scientific Commodities Inc, 0.015" (0.38 mm) I.D. \times 0.043" (1.09 mm) O.D.], which was then inserted into the microchannel after removing air bubbles. The primitive cells in the microfluidic channel were visualized using a Leica microscope (Leica Microsystems, DMI 6000) with a $63\times$ oil-immersion objective. A syringe pump (KD Scientific) was introduced to maintain the flow rate of $0.75\ \mu\text{l}/\text{min}$, $1.5\ \mu\text{l}/\text{min}$, or $3\ \mu\text{l}/\text{min}$.

Videos of the primitive cells flowing through the microchannel were recorded using a high-speed camera (Sample rate: 1900 pps, Phantom) coupled to the Leica microscope. Phantom Camera Control software (PCC) from Vision Research Inc. was used to analyze the elongation of the cell D_l/D_w , where D_l and D_w are the length and width of the cell, respectively. The position of the entrance of the constriction channel is defined as $t = 0\ \text{ms}$. The time frame of cells on corresponding positions was calculated based on the time interval between each frame ($526\ \mu\text{s}$).

C. Preparation of primitive erythroid cell lysates

E12.5 primitive erythroblasts were washed 3 times with phosphate-buffered saline (PBS, 300 mOsm/kg), and then resuspended in RIPA buffer^{30,31} (50 mM Tris [tris(hydroxymethyl)aminomethane], 150 mM NaCl, 1% Nonidet P-40 or 1% Igepal CA-630, Sigma-Aldrich; 0.1% SDS, 0.5% sodium deoxycholate, 1 mM EDTA [ethylenediaminetetraacetic acid], 1 mM DTT [Dithiothreitol], pH 8.0) in the presence of complete protease inhibitor cocktails (Roche), $25\ \mu\text{g}/\text{ml}$ PMSF, and 1 mM Na_3VO_4 , and incubated on ice for 30 min. Nuclei and debris were separated by centrifugation at 500 g for 10 min at 4°C . Samples were stored at -80°C until analysis.

D. Immunoblotting analysis

Erythroid cell lysates from 5×10^{31} cells were separated by 4%–20% SDS-PAGE (Bio-Rad) and transferred to PVDF membranes (EMD Millipore). The membranes were blotted with antibody in 5% (w/v) nonfat dry milk (Bio-Rad) in TBST (50 mM Tris, 150 mM NaCl; 0.1% [v/v] Tween-20), and washed in TBST. The signal was detected using the Pierce ECL Plus Western Blotting Substrate (Thermo Scientific) and developed on a BioMax XAR film (Carestream). Anti-protein 4.1R antibody (NY Blood Center, NY),¹⁴ anti- β -actin antibody (Sigma-Aldrich), and HRP-conjugated secondary antibodies (BioRad) were used in immunoblotting analysis.

E. Cell stain

E10.5 erythroblasts were suspended in 10% Normal Rat Serum (NRS; Invitrogen) and block on ice for 15 min. To stain the cell membrane, 1:100 Alexa Fluor 488-Ter119 (BioLegend) was added on ice for 20 min, followed by one time wash using PB2. Cells were the resuspended in PB2 and stained on ice using DRAQ5 (eBioscience) for another 5 min, after which the cells were ready for imaging.³²

F. Statistics

All data were expressed as mean \pm SD. Unpaired Student's t test was used to compare two different groups. Statistical significance was accepted at $p < 0.05$.

III. RESULTS AND DISCUSSION

We investigated the deformability of primitive erythroblasts by flowing them through a constriction channel ($w_c = 20 \mu\text{m}$, $h = 30 \mu\text{m}$, and $l_c = 100 \mu\text{m}$) embedded in a microfluidic device [Fig. 1(a)]. Because the estimated thoracic aortic shear stress in the embryonic circulation of mouse embryo is about 3.8 Pa,³³ the volumetric flow rates used in the current study were 0.75 $\mu\text{l}/\text{min}$, 1.5 $\mu\text{l}/\text{min}$, and 3 $\mu\text{l}/\text{min}$, which provided approximately shear stresses of 1.05 Pa, 2.1 Pa, and 4.2 Pa, respectively. In Fig. 1(b), $t = 0 \text{ ms}$ was assigned to the time at which the primitive erythroblast entered the constriction channel. An increase of D_l/D_w was observed before $t = 526 \mu\text{s}$, and then D_l/D_w decreased, indicating that the cell elongated upon entering the channel and recovered while exiting the constriction channel [Fig. 1(b)]. The results were consistent with the deformation of mature red blood cells flowing through constriction channels³⁴ and suggested that primitive erythroblasts were deformable at E12.5.

We then studied the effect of flow rate (or shear stress) on the deformation of primitive erythroblasts at two different maturation stages, i.e., E10.5 and E12.5. The results showed that E12.5 cells did not deform significantly when the flow rate was increased from 0.75 $\mu\text{l}/\text{min}$ to 1.5 $\mu\text{l}/\text{min}$. The maximum elongation index, however, increased significantly ($p < 0.0001$) when

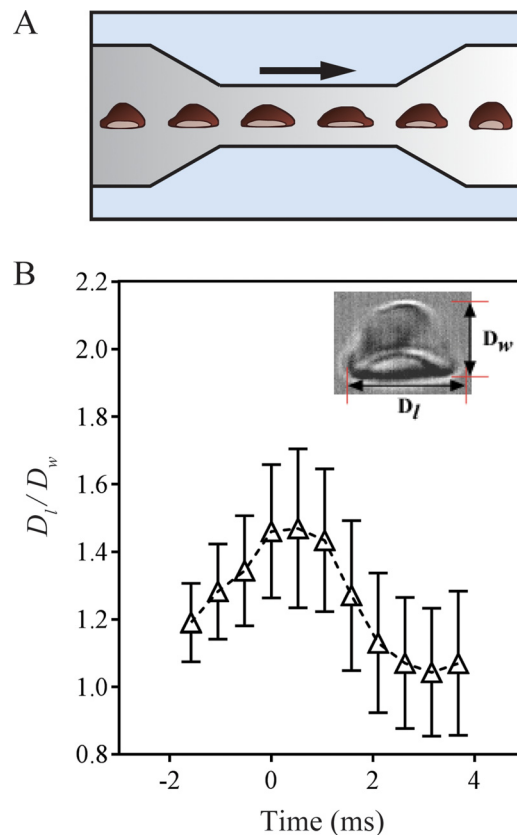


FIG. 1. Experimental setup of the microfluidic assay of the deformability of primitive erythroblasts. (a) Schematic of the microfluidic approach to examine the deformation of primitive erythroblasts. The length (l_c) and width (w_c) of the constriction channel are 100 and 20 μm , respectively. The height of the channel is 30 μm . The arrow indicates the direction of flow. (b) Change of the elongation index (D_l/D_w) of primitive erythroblasts at E12.5 passing through the constriction channel. Flow rate = 1.5 $\mu\text{l}/\text{min}$. Time = 0 ms corresponds to the position of the entrance of the constriction channel. The inset is an image of a primitive erythroblast at E12.5 and the definition of D_l and D_w ($n = 39$).

the flow rate was increased to $3 \mu\text{l}/\text{min}$. Because shear stress at the flow rate of $3 \mu\text{l}/\text{min}$ is approximately 4.2 Pa , close to the estimated shear stress in the embryonic circulation of mouse embryo, the increased elongation index at the flow rate of $3 \mu\text{l}/\text{min}$ demonstrates that E12.5 cells will deform significantly in physiologically relevant flow conditions. As to E10.5 cells [Fig. 2(b)], the elongation index did not show a significant difference when the flow rate increased from $0.75 \mu\text{l}/\text{min}$ to $1.5 \mu\text{l}/\text{min}$. The elongation index started to increase when the flow rate was $3 \mu\text{l}/\text{min}$. To compare the deformability of E12.5 and E10.5 under the same flow rate, we examined the change of the maximum elongation index of both cells. The results showed that E12.5 cells always had a significantly higher elongation index than that of E10.5 cells ($p < 0.0001$) [Fig. 2(c)], indicating that cells at E12.5 were more stretchable than the ones at E10.5. The lack of significant increase of the elongation index with increased shear stress indicated the finite stretchability of E10.5 cells, which might arise from the immature cytoskeletal network or the lack of excess of membrane materials for the given cytoplasmic volume that consequently constrains the deformability of erythroblast cells.

We have shown recently an increased expression of 4.1R transcripts as erythroblast cells transit from E10.5 to E12.5 and that an erythroid-specific isoform switch occurs between E10.5 and E11.5.³² Because 4.1R can form a ternary complex with actin and spectrin and plays important roles in maintaining the integration of the cytoskeletal network of mature erythrocytes,³⁵ it is likely that protein 4.1R in the cytoskeletal composition between E10.5 and E12.5 is,

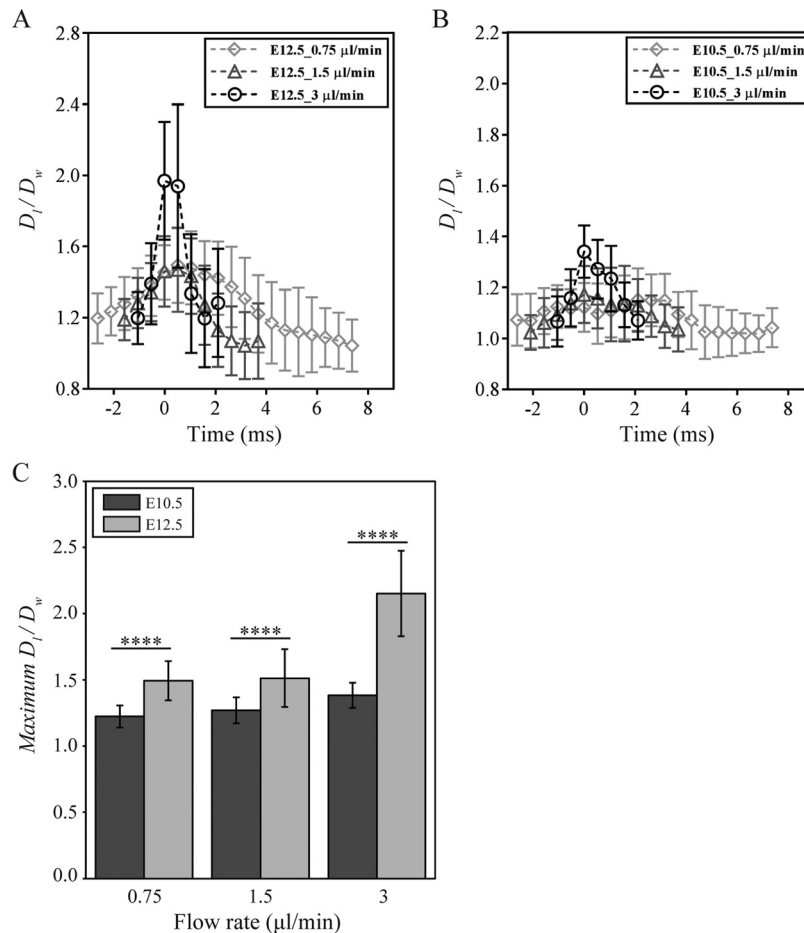


FIG. 2. Effect of flow rates on the change of elongation index of primitive erythroblasts at (a) E12.5 ($n = 173$) and (b) E10.5 ($n = 68$). (c) Effect of flow rates on the change of maximum elongation index (D_f/D_w) of primitive erythroblasts when passing through the constriction channel. The Student's *t*-test showed significant difference between E10.5 and E12.5 cells when applying the same flow rate (****: $p < 0.0001$).

in part, responsible for the observed phenomena in erythroblast cells. To confirm the role of 4.1 R in erythroblast deformability, we tested the shear-induced deformation of primitive erythroblasts from *Epb4.1* knockout (KO) mice. As shown in the Western Blot analysis depicted in Fig. 3(a), control samples with *Epb4.1* *+/+* showed the presence of protein 4.1 R, whereas primitive erythroblasts from *Epb4.1* KO mice lacked the protein 4.1 R. Actin was used as the control to demonstrate that actin was well expressed for both non-KO and KO cells and was detectable. When the deformability of primitive erythroblasts at E12.5 from *Epb4.1* KO mice was studied in the same flow conditions as described above, the elongation index decreased compared to the wild type [Figs. 3(b) and 2(a)]. With the increase of flow rates, the deformation of protein 4.1 KO cells did not change significantly. The E12.5 protein 4.1 KO primitive erythroblasts, in fact, showed similar patterns with E10.5 primitive erythroblasts under the same flow rates [Fig. 2(b)], suggesting that protein 4.1 KO E12.5 cells have the similar deformability as wild type E10.5 primitive erythroblasts. However, when the flow rate increased to 3 $\mu\text{l}/\text{min}$, there was no obvious change in protein 4.1 KO E12.5 cells, while the E10.5 cells can be stretched more under higher shear stress. Because protein 4.1 R is critical to the formation of nodal junctions (with actin and spectrin) of the membrane-skeletal network³⁵ and the maximum local extension of the cell membrane depends on the difference between the average separation of the junctions and the contour length of the spectrin tetramers,³⁶ the lack of 4.1 R in the membrane of erythroblasts likely impairs the connections between spectrin and/or the spectrin dimer-tetramer equilibrium. It attributes to the failure of forming the functional membrane skeleton network.³² A recent study shows that due to the absence of 4.1 R, E12.5 primitive cells cannot transform from spherical to partially concave in shape, leading to a relatively small surface-to-volume ratio,³² which consequently results in decreased cell deformability.^{37,38}

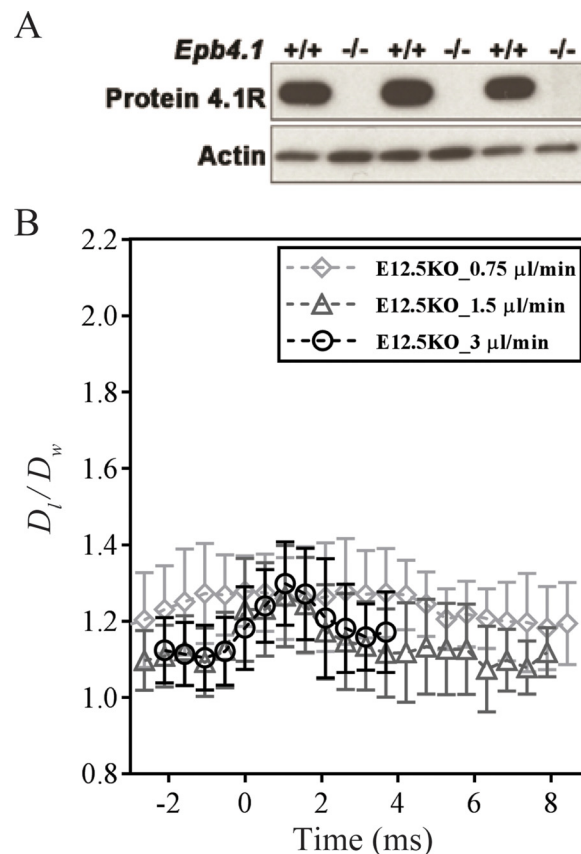


FIG. 3. Effect of 4.1 R on the deformability of primitive erythroblasts. (a) Expressions of cytoskeletal proteins (4.1 R and actin) in knockout (KO) and non-KO E12.5 cells. (b) Effect of flow rates on the elongation index of primitive erythroblasts at E12.5 from *Epb4.1* KO mice ($n = 135$).

Last, to examine the erythroblast deformability in capillaries where cells have to squeeze through the narrow capillary, we flew erythroblasts through a microfluidic device with a much narrower constriction channel that has dimensions of $w_c = 5 \mu\text{m}$, $l_c = 170 \mu\text{m}$, and $h = 7 \mu\text{m}$. In this case, both the membrane and nucleus of the cells are expected to be deformed (Fig. 4). The results showed that, when individual primitive erythroblasts flew through the constriction channel at a constant flow rate ($0.5 \mu\text{l}/\text{min}$), cells at E12.5 could squeeze through the constriction channel without compromising the integrity of the cell, and elongate to almost twice their original length. After exiting the constriction channel, the E12.5 primitive erythroblasts were able to recover their original morphology with a slightly plastic deformation [Fig. 4(a)]. In contrast, when primitive erythroblasts at E10.5 were pushed through the constriction channel, the cells lysed before exiting [Fig. 4(b)]. The results showed that in the conditions of high shear stress and significant deformation, E12.5 cells were more deformable than those of E10.5. It should be noted, however, that the results did not suggest that the nucleus of E12.5 was more deformable than that of E10.5. Although most of the nuclei of E10.5 primitive erythroblasts are lysed while being squeezed inside the constriction channel, (Fig. S1A and B, [supplementary material](#)), there are still some nuclei that are intact after going through the constriction (Fig. S1C, [supplementary material](#)). In addition, it was known that at the late stage of maturation (E12.5-E16.5), interactions between cytoplasmic proteins and the nucleus in primitive erythroblasts are attenuated or lost in

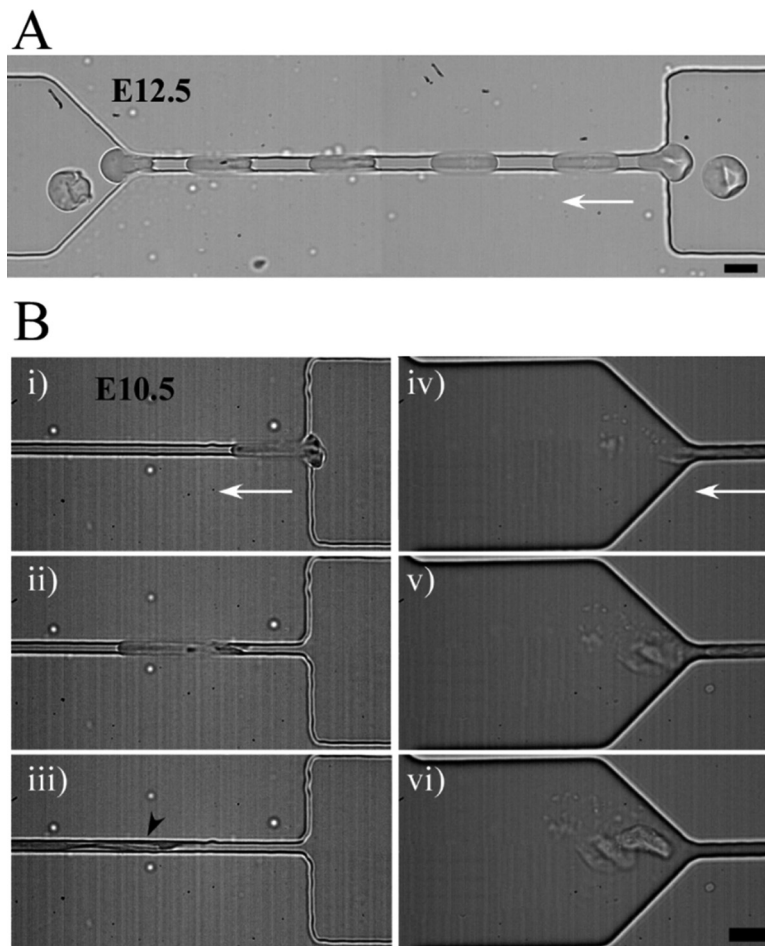


FIG. 4. Deformation of primitive erythroblasts flowing through a narrow microfluidic channel ($l_c = 170 \mu\text{m}$, $w_c = 5 \mu\text{m}$, and $h_c = 7 \mu\text{m}$). The white arrows indicate the flow direction. (a) Superimposed series of time-lapse images showing the deformation of an individual primitive erythroblast at E12.5 passing through a narrow constriction. (b) A sequence of images of primitive erythroblasts at E10.5 flowing through the narrow constriction. Note that the black arrow (iii) indicates the place where cell starts to lyse, and the white arrow indicates the direction of flow. (Scale bar $10 \mu\text{m}$).

preparation for enucleation.^{15,39–41} It is thus possible that the shear force experienced by the membrane of E12.5 cells was not transmitted to the nucleus when passing through the narrow constriction. More importantly, the diameter of primitive erythroblasts decreased from $\sim 15\ \mu\text{m}$ to $13\ \mu\text{m}$ when cells transitioned from E10.5 to E12.5 during embryonic development.¹³ At the same time, the size of nuclei was reduced from $\sim 10\ \mu\text{m}$ for cells at E10.5 to $\sim 5\ \mu\text{m}$ for cells at E12.5 due to nuclear condensation.¹³ With the comparable size of the channel with the size of the nucleus and the deformable membrane of E12.5 primitive cells, the shear force experienced by the E12.5 cells may not be transmitted to the nucleus. Thus, the observed lysis of E10.5 primitive erythroblasts may be due to the decreased membrane deformability and the large size and tethering of the nucleus.

IV. CONCLUSIONS

In summary, by mimicking the physiologically relevant flow conditions using microfluidics, we observed that E12.5 erythroblasts were more deformable than E10.5 erythroblasts under different shear stimulations, and could recover to their original shape after shear-induced deformation. Thus, the deformability of primitive erythroblasts changes during maturation and primitive erythroblasts at late maturational stages are more deformable. This is likely due to the integration of a critical cytoskeletal protein such as protein 4.1R in the membrane at the late maturational stage of primitive erythroblasts. In addition, we demonstrated that the deformability of E12.5 was higher than that of E10.5 when transpassing narrow constrictions with a similar size of capillaries, and thus further supported the notion that the maturity of primitive erythroblasts plays a key role in cell deformation. The findings here provide new insights into the deformation of primitive erythroblasts under flow conditions and are important for understanding the evolution of microcirculation in fetus and how it facilitates the oxygen and nutrition transportation providing the necessary physiological environment.

SUPPLEMENTARY MATERIAL

See [supplementary material](#) for the microscopic images of stained E10.5 erythrocytes before the flow (Fig. S1A), inside the constriction channel (Fig. S1B), and after going through the flow (Fig. S1C).

ACKNOWLEDGMENTS

The authors gratefully acknowledge the support from the Rochester Institute of Technology. This work was supported by the National Institute of Diabetes and Digestive Diseases (DK079361) and the National Heart, Lung and Blood Institute (HL116364) to James Palis. This project was partially supported by the National Science Foundation (CBET-1560709) to Jiandi Wan.

¹K. E. McGrath, A. D. Koniski, J. Malik, and J. Palis, *Blood* **101**, 1669 (2003).

²P. D. Kingsley, J. Malik, K. A. Fantauzzo, and J. Palis, *Blood* **104**, 19 (2004).

³K. E. McGrath, P. D. Kingsley, A. D. Koniski, R. L. Porter, T. P. Bushnell, and J. Palis, *Blood* **111**, 2409 (2008).

⁴J. Malik, A. R. Kim, K. A. Tyre, A. R. Cherukuri, and J. Palis, *Haematologica* **98**, 1778 (2013).

⁵J. Tober, A. Koniski, K. E. McGrath, R. Vemishetti, R. Emerson, K. K. de Mesy-Bentley, R. Waugh, and J. Palis, *Blood* **109**, 1433 (2007).

⁶Z. W. Zhang, J. Cheng, F. Xu, Y. E. Chen, J. B. Du, M. Yuan, F. Zhu, X. C. Xu, and S. Yuan, *IUBMB Life* **63**, 560 (2011).

⁷V. M. Ingram, *Nature* **235**, 338 (1972).

⁸J. Palis and M. C. Yoder, *Exp. Hematol.* **29**, 927 (2001).

⁹K. E. McGrath, J. M. Frame, G. J. Fromm, A. D. Koniski, P. D. Kingsley, J. Little, M. Bulger, and J. Palis, *Blood* **117**, 4600 (2011).

¹⁰J. L. Lucitti, E. A. Jones, C. Huang, J. Chen, S. E. Fraser, and M. E. Dickinson, *Development* **134**, 3317 (2007).

¹¹B. M. Weinstein, *Dev. Dyn.* **215**, 2 (1999).

¹²H. A. Lehr, M. Leunig, M. D. Menger, D. Nolte, and K. Messmer, *Am. J. Pathol.* **143**, 1055 (1993).

¹³S. T. Fraser, J. Isern, and M. H. Baron, *Blood* **109**, 343 (2007).

¹⁴R. E. Waugh, Y. S. Huang, B. J. Arif, R. Bauserman, and J. Palis, *Exp. Hematol.* **41**, 398 (2013).

¹⁵J. C.-M. Lee, J. A. Gimm, A. J. Lo, M. J. Koury, S. W. Krauss, N. Mohandas, and J. A. Chasis, *Blood* **103**, 1912 (2004).

¹⁶T. A. Kalfa, S. Pushkaran, N. Mohandas, J. H. Hartwig, V. M. Fowler, J. F. Johnson, C. H. Joiner, D. A. Williams, and Y. Zheng, *Blood* **108**, 3637 (2006).

- ¹⁷K. B. Hoover and P. J. Bryant, *Curr. Opin. Cell. Biol.* **12**, 229 (2000).
- ¹⁸G. Tchernia, N. Mohandas, and S. Shohet, *J. Clin. Invest.* **68**, 454 (1981).
- ¹⁹J. Conboy, Y. W. Kan, S. B. Shohet, and N. Mohandas, *Proc. Natl. Acad. Sci. U. S. A.* **83**, 9512 (1986).
- ²⁰J. Conboy, N. Mohandas, G. Tchernia, and Y. W. Kan, *New Engl. J. Med.* **315**, 680 (1986).
- ²¹Y. Takakuwa, G. Tchernia, M. Rossi, M. Benabadji, and N. Mohandas, *J. Clin. Invest.* **78**, 80 (1986).
- ²²J. A. Chasis and N. Mohandas, *J. Cell. Biol.* **103**, 343 (1986).
- ²³P. G. Gallagher, paper presented at the Seminars in Hematology (2004).
- ²⁴N. Mohandas, M. R. Clark, B. P. Health, M. Rossi, L. C. Wolfe, S. E. Lux, and S. B. Shohet, *Blood* **59**, 768 (1982).
- ²⁵R. Zhou, J. Gordon, A. F. Palmer, and H. C. Chang, *Biotechnol. Bioeng.* **93**, 201 (2006).
- ²⁶R. Zhou and H. C. Chang, *J. Colloid Interface Sci.* **287**, 647 (2005).
- ²⁷J. Palis and A. Koniski, *Developmental Hematopoiesis* (Springer, 2005), p. 289.
- ²⁸P. D. Kingsley, E. Greenfest-Allen, J. M. Frame, T. P. Bushnell, J. Malik, K. E. McGrath, C. J. Stoeckert, and J. Palis, *Blood* **121**, e5 (2013).
- ²⁹Z.-T. Shi, V. Afzal, B. Coller, D. Patel, J. A. Chasis, M. Parra, G. Lee, C. Paszty, M. Stevens, and L. Walensky, *J. Clin. Invest.* **103**, 331 (1999).
- ³⁰E. Harlow and D. Lane, *Using Antibodies: A Laboratory Manual* (Cold Spring Harbor Laboratory, 1988), p. 579.
- ³¹K. Chen, J. Liu, S. Heck, J. A. Chasis, X. An, and N. Mohandas, *Proc. Natl. Acad. Sci. U.S.A.* **106**, 17413 (2009).
- ³²Y. S. Huang, L. F. Delgadillo, K. H. Cyr, P. D. Kingsley, X. An, K. E. McGrath, M. Narla, J. G. Conboy, R. E. Waugh, J. Wan, and J. Palis, *Sci. Rep.* **7**, 5164 (2017).
- ³³L. B. Langille, *J. Cardiovasc. Pharmacol.* **21**, S11 (1993).
- ³⁴E. Cinar, S. Zhou, J. DeCoursey, Y. Wang, R. E. Waugh, and J. Wan, *Proc. Natl. Acad. Sci. U.S.A.* **112**, 11783 (2015).
- ³⁵M. Salomao, X. Zhang, Y. Yang, S. Lee, J. H. Hartwig, J. A. Chasis, N. Mohandas, and X. An, *Proc. Natl. Acad. Sci. U.S.A.* **105**, 8026 (2008).
- ³⁶D. M. Shotton, B. E. Burke, and D. Branton, *J. Mol. Biol.* **131**, 303 (1979).
- ³⁷Q. Zhu and R. J. Asaro, *Biophys. J.* **94**, 2529 (2008).
- ³⁸X. An, M. C. Lecomte, J. A. Chasis, N. Mohandas, and W. Gratzer, *J. Biol. Chem.* **277**, 31796 (2002).
- ³⁹J. A. Chasis, M. Prenant, A. Leung, and N. Mohandas, *Blood* **74**, 1112 (1989).
- ⁴⁰A. R. Migliaccio, *Haematologica* **95**, 1985 (2010).
- ⁴¹J. Palis, "Regulation red cell life-span, erythropoiesis, senescence and clearance," *Front. Physiol.* **5**, 3 (2014).